

Submitted to Ind. Eng.
Chem. Fundamentals

UCRL-19945
Preprint

c.2

CYCLING ZONE ADSORPTION:
QUANTITATIVE THEORY AND EXPERIMENTAL RESULTS

RECEIVED
LAWRENCE
RADIATION LABORATORY

Burke Baker, III and Robert L. Pigford

SEP 17 1970

July 1970

LIBRARY AND
DOCUMENTS SECTION

AEC Contract No. W-7405-eng-48

TWO-WEEK LOAN COPY

*This is a Library Circulating Copy
which may be borrowed for two weeks.
For a personal retention copy, call
Tech. Info. Division, Ext. 5545*

LAWRENCE RADIATION LABORATORY
UNIVERSITY of CALIFORNIA BERKELEY

UCRL-19945 c.2

DISCLAIMER

This document was prepared as an account of work sponsored by the United States Government. While this document is believed to contain correct information, neither the United States Government nor any agency thereof, nor the Regents of the University of California, nor any of their employees, makes any warranty, express or implied, or assumes any legal responsibility for the accuracy, completeness, or usefulness of any information, apparatus, product, or process disclosed, or represents that its use would not infringe privately owned rights. Reference herein to any specific commercial product, process, or service by its trade name, trademark, manufacturer, or otherwise, does not necessarily constitute or imply its endorsement, recommendation, or favoring by the United States Government or any agency thereof, or the Regents of the University of California. The views and opinions of authors expressed herein do not necessarily state or reflect those of the United States Government or any agency thereof or the Regents of the University of California.

CYCLING ZONE ADSORPTION: *
QUANTITATIVE THEORY AND EXPERIMENTAL RESULTS

Burke Baker, III[†] and Robert L. Pigford

Department of Chemical Engineering
and Lawrence Radiation Laboratory
University of California
Berkeley, California 94720

July 1970

ABSTRACT

A theoretical explanation for cycling zone adsorption, a wave-propagational separation process given a qualitative explanation in an earlier article, is presented. Experimental results confirming the theoretical predictions are also included. It is found that in addition to accounting for the separation effect the theory predicts the effect can be amplified through the interaction of the concentration and progressing thermal waves. Possible process schemes utilizing the interaction are discussed.

INTRODUCTION

In a recent article by Pigford, Baker, and Blum (1969b) a qualitative description was presented of a cyclic fixed-bed separation process given the name "cycling zone adsorption." The first objective of this article will be to explain the process, theoretically. This leads to certain predictions of ways of introducing heat into the bed that will increase the concentration change. Finally, experimental evidence of the predictions is offered.

Consider the process shown in Fig. 1a or Fig. 1b in which a fluid having a constant solute concentration, y_f , is passed through a bed of solid particles. The temperature of the bed is cyclically altered, either by heating and cooling

[†]Present Address: Shell Oil Co., Deer Park, Texas.

the walls, as in Fig. 1a (standing thermal wave), or by using a pre-exchanger to heat and cool the input stream as in Fig. 1b (travelling thermal wave). As explained in the earlier article, cyclic changes in the effluent concentration are obtained; these changes can be amplified by using a series of such columns.

MATHEMATICAL MODEL

The equations governing the process are those for a non-isothermal, fixed-bed system which are derived from mass and heat balances over each phase. Disregarding radial gradients in velocity, concentration and temperature, the balances for a packed column through which a solution containing a single adsorbate is flowing yield (Baker, 1969)

$$\frac{\partial c}{\partial t} + \frac{(1-\alpha)\epsilon}{\alpha} \frac{\partial c^*}{\partial t} + \rho_s \frac{(1-\alpha)(1-\epsilon)}{\alpha} \frac{\partial q}{\partial t} + v \frac{\partial c}{\partial z} - (E_D + D_M) \frac{\partial^2 c}{\partial z^2} = 0 \quad (1)$$

$$\begin{aligned} \frac{\partial T}{\partial t} + \frac{\rho_s C_s (1-\epsilon) + \rho_f C_f \epsilon}{\rho_f C_f \alpha} (1-\alpha) \frac{\partial T_s}{\partial t} + v \frac{\partial T}{\partial z} \\ - (E_D + D_T) \frac{\partial^2 T}{\partial z^2} = \frac{h_w a_w}{\rho_f C_f \alpha} (T_w - T) \end{aligned} \quad (2)$$

$$\frac{\partial q}{\partial t} + \frac{\epsilon}{\rho_s (1-\epsilon)} \frac{\partial c^*}{\partial t} = - \frac{k_M a_p}{\rho_s (1-\epsilon)(1-\alpha)} (c^* - c) \quad (3)$$

$$\begin{aligned} \frac{\partial T_s}{\partial t} = - \frac{h_p a_p}{[\rho_s C_s (1-\epsilon) + \rho_f C_f \epsilon](1-\alpha)} (T_s - T) \\ + \frac{(1-\epsilon) \rho_s \Delta H_{ads}}{[\rho_s C_s (1-\epsilon) + \rho_f C_f \epsilon]} \frac{\partial q}{\partial t} \end{aligned} \quad (4)$$

where α = fraction of the packed bed outside the adsorbent particles and ϵ = fraction by volume of immobile fluid inside the particles.

The interface between the surface of the solid and the fluid inside the solid particles is considered to be at equilibrium and is represented by an expression of the type

$$q = q(T_s, c^*) . \quad (5)$$

Any effect of temperature on the parameters has been neglected except in the equilibrium relationship. The assumption of over-all linear driving-force relationships for the mass transfer (Sweed and Wilhelm, 1969) may not be precisely true in some cases and may need to be replaced by the corresponding radial intra-particle diffusion terms. For slow transfer, however, the simpler expressions are sufficient. In the equations the stationary phase is treated in two parts, the adsorbent itself (concentration = q) and the immobile fluid in the pores (concentration = c^*), assumed to be in local equilibrium with the adsorbent.

Since the separation effect in the process depends on a cyclic alteration in the phase equilibrium rather than on any rate differences, the approach taken in this study was first to design what is a good process based on the equilibrium theory, assuming that rates of exchange are very high, and then to develop the mass and heat relationships for the general case in which rates may be important. If it is assumed that at any point in the column the solid and fluid phases are in equilibrium, i.e., $c = c^*$ and $T_s = T$, and that axial dispersion and heat of adsorption effects may be neglected, an analytic solution to the simplified equations is possible. This is presented below. (The Freundlich

isotherm,

$$q = A (c^*)^k; \quad 0 < k \leq 1, \quad (6)$$

will be used later in Eq. (5) since it will apply to the experimental system discussed below.)

Using dimensionless dependent variables, the equations, which have been simplified using the above assumptions,

$$\left[1 + \frac{1-\alpha}{\alpha} \epsilon + \frac{1-\alpha}{\alpha} (1-\epsilon) \rho_s \left(\frac{\partial q}{\partial c}\right)\right] \frac{\partial c}{\partial t} + v \frac{\partial c}{\partial z} = - \frac{1-\alpha}{\alpha} (1-\epsilon) \rho_s \left(\frac{\partial q}{\partial T_s}\right) \left(\frac{\partial T}{\partial t}\right) \quad (7)$$

$$\frac{\partial T}{\partial t} + u_{th} \frac{\partial T}{\partial z} = 0 \quad (8)$$

Assuming that the temperature of the column is changed by changing the temperature of the feed stream, the boundary conditions are

$$C = C_0; \quad z = 0, \quad t > 0$$

$$T = T_0 + (T_H - T_0) \text{sq}(\omega t); \quad z = 0, \quad t > 0$$

i.e., the inlet temperature is cycled in a square wave of frequency $\omega/2\pi$ cycles/sec. The solution to equation 8 is

$$T - T_0 = (T_H - T_0) \text{sq}(\omega t - \omega z/u_{th}), \quad (9)$$

representing the propagation of temperature through the bed as a traveling wave of velocity u_{th} . If the column is heated and cooled through the walls, this

natural thermal velocity is overridden; then a standing temperature wave is produced and, effectively, $u_{th} \rightarrow \infty$.

The occurrence of the independent variables in the combination $t - z/u_{th}$ suggests a change to the new independent variables

$$\tau = t - z/u_{th}$$

$$\zeta = z$$

$$\begin{aligned} & \left[1 + \frac{1-\alpha}{\alpha} \epsilon + \frac{1-\alpha}{\alpha} (1-\epsilon) \frac{\partial(q\rho_s)}{\partial c} - \frac{v}{u_{th}} \right] \frac{\partial c}{\partial \tau} + v \frac{\partial c}{\partial \zeta} \\ & = \frac{1-\alpha}{\alpha} (1-\epsilon) \frac{\partial(q\rho_s)}{\partial T_s} \left(\frac{\partial T}{\partial \tau} \right) \end{aligned} \quad (10)$$

with the boundary and forcing conditions:

$$c = c_0 ; \zeta = 0, \tau > 0$$

$$T = T_0 + (T_H - T_0) \text{sq}(\omega\tau) ; \zeta = 0, \tau > 0$$

Using the method of characteristics as in Pigford et al. (1969a), Eq. (10) is equivalent to the pair of ordinary equations

$$\frac{d\zeta}{1} = \frac{d\tau}{1 + \frac{1-\alpha}{\alpha} \epsilon + \frac{1-\alpha}{\alpha} (1-\epsilon) \frac{\partial(q\rho_s)}{\partial c} - \frac{v}{u_{th}}} = \frac{-dc}{\frac{1-\alpha}{\alpha} (1-\epsilon) \frac{\partial(q\rho_s)}{\partial T_s} \frac{dT}{dt}} \quad (11a,b)$$

Solutions to Eq. (11a) are lines in the $\tau - \zeta$ characteristics. Solutions to Eq. (11b), yielding c as a function of τ , are valid only along these characteristics. If the temperature is constant ($\partial T/\partial \tau = 0$), the solution to Eq. (11b) is

$$\left[1 + \frac{1-\alpha}{\alpha} \varepsilon - (v/u_{th})\right]c + \frac{1-\alpha}{\alpha} (1-\varepsilon) \rho_s q = \text{constant} \quad (12)$$

Thus, c remains constant along a characteristic, except when the temperature changes. When the temperature is switched, the concentration changes can be expressed as

$$\left[1 + \frac{1-\alpha}{\alpha} \varepsilon - (v/u_{th})\right](c_{i+1} - c_i) + \frac{1-\alpha}{\alpha} (1-\varepsilon) \rho_s (q_{i+1} - q_i) = 0 \quad (13)$$

from Eq. (12), where $i-1$ refers to conditions before the switch and i to conditions afterwards.

Defining the concentration velocity as

$$u_c(c, T) = \frac{v}{1 + \frac{1-\alpha}{\alpha} \varepsilon + \frac{1-\alpha}{\alpha} (1-\varepsilon) \rho_s (\partial q / \partial c)} \quad (14)$$

Equation (14) can be expressed as

$$\frac{d\zeta}{d\tau} = \left(\frac{v}{u_c} - \frac{v}{u_{th}}\right)^{-1} \quad (15)$$

showing that the slope of a characteristic path line depends both on temperature and local concentration.

LINEAR ISOTHERM:

In the event $k = 1$, i.e., if the Freundlich isotherm is straight, u_c is concentration-independent. Equation (13) reduces to

$$\frac{c_i}{c_{i-1}} = \frac{u_{c,i-1}^{-1} - u_{th}^{-1}}{u_{c,i}^{-1} - u_{th}^{-1}} \quad (16)$$

Since in nearly all adsorption systems solute is rejected from the solid when the system temperature is raised, $u_c^C < u_c^H$ and

$$c_c/c_H = Q < 1 .$$

A solution for this linear case is shown in Fig. 2.

When a characteristic passes from a warm region into a cold one, the concentration along it changes by the ratio, Q . When a characteristic passes from a cold region into a warm one, the concentration changes by the ratio $Q - 1$.

It is now clear why there is an optimum cycling frequency. If the frequency is too low, there will be too many characteristics undergoing no temperature change and the fluid will leave the column at the feed concentration, c_0 . If the frequency is too high, too many characteristics will undergo two temperature changes and again emerge with concentration, y_0 . To find the optimum, the concentrations are averaged over each half cycle and the average separation factor, α_{av} , is computed. The fractions $(ab + cd)/ad$ and bc/ad must be found from the slopes of the characteristics in the figure. These are

$$\left. \begin{array}{l} \frac{bc}{ad} = Q \\ \frac{ab + cd}{AD} = -Q \end{array} \right\} \text{for } \frac{1}{u_c^C} - \frac{1}{u_{th}} \geq \frac{\pi}{\omega} \geq \frac{1}{u_c^H} - \frac{1}{u_{th}} ,$$

and, therefore,

$$\langle c_l \rangle = c_0 Q$$

$$\langle c_h \rangle = c_0 (1-Q) + c_0 Q^{-1} \cdot Q = c_0 (2-Q)$$

$$\alpha_{av} \equiv \frac{\langle c_h \rangle}{\langle c_l \rangle} = \frac{2-Q}{Q} .$$

Therefore α_{av} has a constant optimum value in this range and a lower value for frequencies outside of this range.

For the multiple zones, the same solution holds for the individual zones as shown in Fig. 3. In the figure, phase lag was chosen to be π and the frequency chosen so that $\pi/\omega = 1/(1/u_c^c - 1/u_{th})$. The fractions ab/ac and bc/ac are similar to the previous case. This results in the difference equations

$$\langle c_h \rangle_n = \langle c_l \rangle_{n-1} (1 - Q) + \langle c_h \rangle_{n-1} Q^{-1} \cdot Q , \quad (17a)$$

$$\langle c_l \rangle_n = \langle c_l \rangle_{n-1} \cdot Q , \quad (17b)$$

where n is the zone number, the boundary conditions being

$$\langle c_h \rangle_0 = \langle c_l \rangle_0 = c_0 .$$

The solution to Eq. (2-21b) is

$$\langle c_l \rangle_n = c_0 Q^n , \quad (18)$$

which, inserted in Eq. (17a), results in

$$\langle c_h \rangle_n = [1 + (1-Q) \sum_{i=0}^{n-1} Q^i] c_0 = [2 - Q^n] c_0 , \quad (19)$$

and

$$\alpha_{av,n} = \frac{2 - Q^n}{Q^n} \quad (20)$$

This predicts that as $n \rightarrow \infty$, all of the solute introduced with the feed comes out during the hot cycle and that the effluent during the cold cycle has zero concentration. The average concentration during the hot cycle must be limited to twice the feed concentration, but there is no limitation to the peak value of the concentration.

This is one obvious defect of the linear-isotherm assumption. Physically, the preferential isotherm for any system must go to zero, both at zero solute concentration and at 100 per cent solute, so that no isotherm can remain linear over the whole range of concentration.

For $u_{th} = \infty$, i.e., for standing thermal waves, Eq. (20) is the same result that was obtained for the batch form of direct-mode (jacketed column) parametric pumping by Pigford et al. (1969a). For parametric pumping, n refers not to zone number but to the number of flow-reversal cycles experienced by one zone. The important difference to be noted is that in cycling zone adsorption, production is realized at fluid velocity v , whereas in the comparable parametric pumping experiment there was no feed and therefore no production.

NON-LINEAR ISOTHERM:

Using the fact that c remains constant along a characteristic between temperature switches, Eqs. (6) and (13) are solved at each temperature switch, using a non-linear, algebraic, root-finding procedure such as Newton's method, to give boundary conditions along the ζ -axis at the beginning of each half cycle. For Eq. (11a) the feed condition at $\zeta = 0$ is the other required boundary condition. This is similar to the standard isothermal non-linear adsorption problem treated by Goldstein (1953).

Since the characteristics are concentration-dependent there will be regions of sharp "shock-wave" concentration fronts, and of diffuse fronts called "simple waves." The results for a single-zone column are shown in Fig. 4. A shock wave occurs in the cold half-cycle when fluid of lower concentration, $c_i < c_0$, is being displaced by feed, $c = c_0$. The shock velocity (Baker, 1969) is

$$u_{sh} = v / \left[1 + \frac{1-\alpha}{\alpha} \epsilon + \frac{1-\alpha}{\alpha} (1-\epsilon) m_i \frac{1 - \bar{y}_i^{k_i}}{1 - \bar{y}_i} \right], \quad (21)$$

where i refers to cold half-cycle parameters, $m = (\rho_s/A)c_0^{1-k}$, and $\bar{y} = c/c_0$. A simple wave occurs during the hot half-cycle when fluid of higher concentration, $c_i > c_0$ is being displaced by feed. The concentrations are

$$\zeta > \tau/g(y_i); \quad c = c_i, \quad (22)$$

$$\zeta > \tau/g(1); \quad c = c_0, \quad (23)$$

$$\tau/g(1) < \zeta < \tau/g(y_i); \quad c = \frac{(\tau/\zeta) - (1 + \frac{1-\alpha}{\alpha} \epsilon - \frac{v}{u_{th}})}{(1-\alpha)(1-\epsilon)m_i y_i / \alpha} c_0, \quad (24)$$

where

$$g(y) = 1 + \frac{1-\alpha}{\alpha} \epsilon - \frac{v}{u_{th}} + \frac{1-\alpha}{\alpha} (1-\epsilon) k_i m_i y_i^{k_i-1},$$

and i refers to the hot half-cycle parameters.

In the multiple zone arrangement, as these long sections of lean and enriched fluid are sent through successive columns, shock waves remain relatively sharp but the simple waves become more and more diffuse. Since the

concentration differences are being progressively increased, this effect is amplified as the separation progresses. Eventually the leading-edge of the simple wave overtakes the shock wave and diminishes the peak concentration. This is what keeps the concentration peak from becoming infinite. A general solution for n zones in the non-linear case would be difficult but the dual-zone case is shown in Fig. 4. Zone 2 has received the effluent from zone 1, cf. Fig. 2.

AMPLIFICATION BY ADJUSTING THE THERMAL WAVE VELOCITY

One notes that the concentration shift relationship, Eq. (13), depends on u_{th} . Suppose a thermal wave of arbitrary velocity could be imposed on the system, overriding the natural thermal wave, as in the standing wave case. Some experimental proposals for this will be discussed later. For linear isotherms (u_c not dependent on y):

A. For $u_{th} > u_c^H > u_c^C$,

$$y_i \rightarrow 0; (i = \text{cold}, i-1 = \text{hot}) \text{ (cold wave)}$$

and

$$y_i \rightarrow \infty; (i = \text{hot}, i-1 = \text{cold}) \text{ (hot wave)}$$

as

$$u_{th} \rightarrow u_c^H > u_c^C, y_{i-1} \neq 0$$

B. For $u_c^H > u_c^C > u_{th}$,

$$y_i \rightarrow 0; (i = \text{hot}, i-1 = \text{cold}) \text{ (cold wave)}$$

and

$$y_i \rightarrow \infty; (i = \text{cold}, i-1 = \text{hot}) \text{ (hot wave)}$$

as

$$u_{th} \rightarrow u_c^C < u_c^H, y_{i-1} \neq 0$$

These relationships are shown in Fig. 5 on $t - z$ coordinates. Combining these two cases,

$$C. \text{ For } u_c^H > u_{th} > u_c^C$$

$$y_i \rightarrow 0 \text{ (cold wave)}$$

$$y_i \rightarrow \infty \text{ (hot wave) ,}$$

as in Fig. 5. As before, the predictions of an infinite concentration is a limitation of the linear isotherm; a consideration of the non-linear case shows that the simple wave will overtake the shock wave and keep the maximum concentration finite.

The prediction of this large amplification in the separation effect, caused by the interaction of the thermal and concentration waves as their velocities approach the same value, is similar to the compression effect first reported by Zhukhovitskii et al. (1951) in the process he called "chromatography." There, a conventional gas chromatograph was modified by having a mobile external furnace. The furnace produced a travelling temperature gradient and moved along the column at such a speed that each solute to be

separated had its concentration at the coldest temperature smaller than the furnace velocity but that at the hottest temperature greater than the furnace velocity. Thus the peak for each solute tended to be compressed around a particular temperature for which the concentration velocity was equal to the furnace velocity. In this way, a concentration of solute in excess of the input concentration was produced as well as a separation from the other solutes (Tudge, 1961 and Ohline and De Ford, 1963).

There has been no effort so far to test the travelling wave effect in cycling zone adsorption. Use of an external furnace is probably not practical for full-scale processes as liquid-solid systems, even though it has worked in the chromathermography process for gas-solid analytical scale systems (Zhukhovitskii, 1960). Alternate schemes of either slowing down the natural thermal wave (by adding wall heat capacitance) or speeding up the concentration wave (by adding inert solid) should be tried.

It is important to note that, in a sense, the multiple zone version of cycling zone adsorption is a finite-zone approximation of the smooth travelling-wave effect. Each zone is cycled π radians (one-half cycle) out of phase with the preceding zone; the effect is to produce a stair-step thermal wave which moves through the zones. For a constant total length, as the length of the individual zones decreases the number of zones increases. In the limit, the stair-step wave becomes a smooth travelling thermal wave having a velocity equal to the concentration velocity. Thus, cycling zone adsorption, with use of inter-column exchangers is a physically practical way of implementing the thermal wave propagational effect.

EXPERIMENTAL SYSTEM

To demonstrate the process, the separation of acetic acid from water on activated carbon was selected because the shift of the equilibrium distribution relationship with temperature and the intra-particle mass transfer rate were reasonably large. Also, effluent concentrations could easily be monitored continuously using an electrical conductivity cell and intermittantly checked by acid-base titration. The preferential adsorption isotherms were determined and fitted to a Freundlich isotherm; the parameters are shown in Table I.

Table I. Freundlich Equilibrium Distribution Parameters^a

Temperature, °C	A	k
4	3.646	0.3052
60	3.019	0.4119

^aThe units of A are (moles/liter dry carbon)·(liters/mole)^k; k has no units.

The strong curvature of the isotherms required the non-linear analysis presented earlier. The essential parameters of the bed are presented in Table II.

Table II. Activated Carbon Physical Parameters

	Mesh size		Units
	20-40	50-140	
Structural density, ρ_s	1.728	1.820	g/cm^3
Particle density, $\rho_s \cdot \epsilon$	0.8018	0.7822	g/cm^3
Intraparticle void fraction, ϵ	0.5360	0.5702	-
Interparticle ^a void fraction, α	.438-.473	.426-.443	-
Particle diameter, d_p	.420-.841	.105-.297	mm
Heat capacity, ^b C_s	0.25	0.25	$\text{cal/g-}^\circ\text{C}$

^a Depending on particular experiment.

^b Supplied by manufacturer.

THE EXPERIMENTAL APPARATUS:

The apparatus can be divided into sections:

The column section had various arrangements to test several process ideas as shown in Fig. 6. Each glass column was 1.9 cm by 26 cm and was packed at the top and bottom with 0.1-cm glass spheres for flow distribution. Polyurethane foam insulation was used, limiting the radial heat loss to about 10% of that supplied to the bed. The water jackets were standard laboratory condenser jackets. The pre-exchangers were similar to the columns but were 12.5 cm long and were packed with glass spheres. The feed was taken from a 13-gal. reservoir which was pressurized with air when gravity feed provided insufficient flow.

The thermal-forcing section produced square temperature waves using a system of hot and cold water reservoirs and solenoid valves. Frequency and phase were varied manually and with a repeat-cycle timer.

The measurement system monitored temperature using thermocouples in the inlet and outlet streams and effluent concentration using an electrical conductivity flow cell and bridge circuit. The effluent was cooled to a constant temperature before passing through the cell. Because of the non-linear conductivity-concentration relationship, intermittent sampling and acid-base titration was also used. Average concentrations were determined by planimeter integration.

EXPERIMENTAL RESULTS:

The experimental results are presented here to show the feasibility of the process and the enhanced separation gained by multiple zoning. The non-linear, equilibrium theory is applied to the fine carbon particles (50-140 mesh) to determine to what extent the observed concentration wave distortion can be accounted for.

SINGLE ZONE EXPERIMENTS:

The single-zone experiment shown in Fig. 7 with the temperature profile of Fig. 11 is the base experiment with which others are compared. The peak values are somewhat overestimated by the theory; this may be due to a deactivation of the carbon after repeated cycling. Some dispersion is also evident; this is due to an intra-particle, diffusion-limited mass transfer resistance. Two rather obvious results, observed but not illustrated, are that increasing the amplitude of the temperature shift increases the separation and that increasing the particle size decreases the concentration maxima.

Figure 8 illustrates two important considerations in the design of a cycling zone adsorption process.

1) In this example of a highly non-linear system, the wave velocities are very different in the three concentration ranges. Thus the greater the separation one is able to obtain in the system, the larger will be the difference in concentration velocities during each half cycle. This suggests that some recycle arrangement may be necessary in these cases.

2) In this system, the isotherms at the upper and lower temperatures intersect at about 5-N. One observes that the separation decreases rapidly as the feed approaches this concentration. This is analogous to an azeotrope in distillation and places an upper limit on the concentration that can be achieved using this adsorbent.

The results in Fig. 9 substantiate the prediction of an optimal cycling frequency, which produces the maximum average separation factor. The effect of the limitation in mass-transfer rate is also evident in the attenuation of the peak separation factor; this is not predicted by equilibrium theory.

The comparison of temperature response for the standing and travelling wave experiments is shown in Fig. 10. The slight attenuation in the outlet amplitude is caused by radial heat loss. The curvature in the outlet response is almost entirely owing to curvature in the inlet response; little thermal dispersion took place. Only the hot wave is shown; the cold wave is simply the inverse. The predicted curves are plotted from Eq. (9) with u_{th} calculated from the heat capacities and densities of the solid, liquid, and glass wall; the heat loss is not considered. Figure 10 shows the effluent concentration history.

The thermal-forcing section produced square temperature waves using a system of hot and cold water reservoirs and solenoid valves. Frequency and phase were varied manually and with a repeat-cycle timer.

The measurement system monitored temperature using thermocouples in the inlet and outlet streams and effluent concentration using an electrical conductivity flow cell and bridge circuit. The effluent was cooled to a constant temperature before passing through the cell. Because of the non-linear conductivity-concentration relationship, intermittent sampling and acid-base titration was also used. Average concentrations were determined by planimeter integration.

EXPERIMENTAL RESULTS:

The experimental results are presented here to show the feasibility of the process and the enhanced separation gained by multiple zoning. The non-linear, equilibrium theory is applied to the fine carbon particles (50-140 mesh) to determine to what extent the observed concentration wave distortion can be accounted for.

SINGLE ZONE EXPERIMENTS:

The single-zone experiment shown in Fig. 7 with the temperature profile of Fig. 11 is the base experiment with which others are compared. The peak values are somewhat overestimated by the theory; this may be due to a deactivation of the carbon after repeated cycling. Some dispersion is also evident; this is due to an intra-particle, diffusion-limited mass transfer resistance. Two rather obvious results, observed but not illustrated, are that increasing the amplitude of the temperature shift increases the separation and that increasing the particle size decreases the concentration maxima.

Figure 8 illustrates two important considerations in the design of a cycling zone adsorption process.

1) In this example of a highly non-linear system, the wave velocities are very different in the three concentration ranges. Thus the greater the separation one is able to obtain in the system, the larger will be the difference in concentration velocities during each half cycle. This suggests that some recycle arrangement may be necessary in these cases.

2) In this system, the isotherms at the upper and lower temperatures intersect at about 5-N. One observes that the separation decreases rapidly as the feed approaches this concentration. This is analogous to an azeotrope in distillation and places an upper limit on the concentration that can be achieved using this adsorbent.

The results in Fig. 9 substantiate the prediction of an optimal cycling frequency, which produces the maximum average separation factor. The effect of the limitation in mass-transfer rate is also evident in the attenuation of the peak separation factor; this is not predicted by equilibrium theory.

The comparison of temperature response for the standing and travelling wave experiments is shown in Fig. 10. The slight attenuation in the outlet amplitude is caused by radial heat loss. The curvature in the outlet response is almost entirely owing to curvature in the inlet response; little thermal dispersion took place. Only the hot wave is shown; the cold wave is simply the inverse. The predicted curves are plotted from Eq. (9) with u_{th} calculated from the heat capacities and densities of the solid, liquid, and glass wall; the heat loss is not considered. Figure 10 shows the effluent concentration history.

The estimate of u_{th} given above was again used for the travelling wave case. The slightly beneficial effect of having a travelling wave instead of a standing wave can be noticed, even though u_{th} was much larger than the concentration velocities.

The main points to be observed are that the travelling-wave method is efficient and the separation is as good or better than that obtained with standing thermal waves. Moreover, the efficiency should not decrease as the diameter of the column increases, as with external heating and cooling.

DOUBLE-ZONE EXPERIMENTS:

The two-zone standing-wave experiment reported by Pigford et al. (1969) is again shown in Fig. 11, this time with the equilibrium-theory predictions. The correct low concentration is predicted, but the high-concentration peak is narrow enough to have been considerably modified by dispersion. The fact that the concentration waves are non-linear (concentration dependent) is important here. Because the high-concentration peak from the first zone travels faster than, for example, the feed concentration, this peak can pass through the second zone and out before the zone is raised to the high temperature. Thus it never gets shifted to higher concentration. To obtain this shift, the cycle frequency for the second zone would have to be higher than that of the first. Nevertheless, the beneficial effect of multiple zoning is evident from the separation factors.

The following studies were made with larger particles of 20-40 mesh carbon. The prediction of an optimum cycling frequency for the two-zone case was confirmed. The prediction of an optimum in the phase lag between the temperature forcing of the two columns was also substantiated. Baker (1969) showed that the optimum phase lags giving the maximum in α_{av} and

α_{pk} are not exactly at 180° , as expected from the linearized theory but approximate the values found experimentally. Finally, Fig. 12 shows the success of travelling-wave forcing in the dual-zone process.

DISCUSSION AND CONCLUSIONS

It has been demonstrated theoretically and on a laboratory scale that the cycling zone adsorption process is feasible. Significant separations are predicted mathematically using the equilibrium theory, at least when the isotherms are not too strongly curved. Significant but by no means complete separations were observed. Particularly evident was the predicted increase in separation power gained by using multiple zones in series. Furthermore, the cyclic transfer of thermal energy in and out of the zones, which is essential to the process, can be accomplished very efficiently in liquid-solid systems by the use of the natural thermal, travelling-wave properties of the zones.

Certain difficulties are evident. The small shift in the equilibrium isotherm for moderate temperature changes indicates that several zones will be required for significant separation. This means additional thermal requirements. Internal reuse of the heat is possible; the feasibility of an inter-stage heat regenerator has been discussed by Baker (1969). The experimental results and perturbation theory predictions indicate that low mass-transfer rates attenuate the separation from the equilibrium theory predictions. This means that for these intra-particle diffusion-controlled systems, one must operate at low flow rates or with fine particles, thus restricting the throughput possible.

The presence of dispersion, caused by the non-linear isotherms and finite transfer rates may require recycle arrangements. One may want to collect

the effluent only during the emergence of the high and low peaks, returning the rest to the feed stream to be returned to the column at the proper time in the cycle. This would increase equipment and operating costs, however.

The practicality of imposing travelling waves on this type of system remains to be demonstrated, although it has been done in analytical gas chromatography. If it should not prove to be feasible for thermal waves, it should be kept in mind that the effect would occur for any intensive variable that can shift the solid-fluid equilibrium. Certain such variables, for example electrical or magnetic fields may be easier to use as travelling waves, thus amplifying a small separation effect.

Cycling zone adsorption is an attractive process which may economically perform the intermediate scale separation of material which now must be separated chromatographically.

ACKNOWLEDGMENTS

We thank the Pittsburgh Activated Carbon Co. for donating the carbon for this study.

Studies supported by AEC Contract W-7405-eng-48. Additional support through NASA Predoctoral Traineeship ASG(T)-117-2 and a Shell Companies Foundation Fellowship was provided to one of the authors.

NOMENCLATURE (Dimensionless unless specified)

- A = solid-fluid equilibrium distribution parameter, units depend on function.
- D_M = mass molecular diffusivity, cm^2/min .
- D_T = thermal molecular diffusivity, cm^2/min .
- E_D = eddy axial dispersion, cm^2/min .

- ΔH_{ads} = differential heat of adsorption, cal/mole.
- R = gas constant, cal/(gmole)(°C).
- T = temperature, °C.
- Z_0 = length of bed, cm.
- a = surface area/bed volume ratio, cm^{-1} .
- c = fluid concentration, moles/liter.
- c^* = fluid concentration in equilibrium with solid-phase concentration, moles/liter.
- h = heat transfer coefficient, $cal/(cm^2)(min)(°C)$.
- k = exponent in Freundlich isotherm.
- q = solid-phase concentration, moles/kg dry solid.
- t = time, min.
- u = wave velocity.
- v = interstitial fluid velocity, cm/min.
- y = c/c_0 , concentration in fractions of feed concentration.
- z = axial distance, cm.
- α = interparticle void fraction.
- α_{pk} = $y_{h,pk}/y_{l,pk}$, peak separation factor.
- α_{av} = $\langle y_h \rangle / \langle y_l \rangle$, cycle-averaged separation factor.
- ϵ = intra-particle void fraction.

- ρ_s = structural density of solid, kg/cm^3 .
- τ = $t-z/u_{th}$, time, sec.
- ω = frequency, radians/min.
- ζ = distance, cm.

SUBSCRIPTS

- w refers to tube wall surrounding the system.
- C = cold.
- c = concentration-related value.
- f = feed condition.
- H = hot.
- h = high.
- i+1 = conditions after a concentration characteristic crosses a temperature boundary.
- i = conditions before a concentration characteristic crosses a temperature boundary; if i = hot, i-1 = cold, and vice versa.
- l = low.
- s = solid.
- th = thermal.

SUPERSCRIPTS

- C = cold.
- H = hot.

LITERATURE CITED

- Baker, B. III, Ph.D. dissertation, University of California, Lawrence Radiation Laboratory, Berkeley, 1969.
- Goldstein, F. R. S., Proc. Roy. Soc. A219, 151 (1953).
- Online, R. W., and DeFord, D. D., Anal. Chem. 35, 227 (1963).
- Pigford, R. L., Baker, B. III, Blum, D. E., Ind. Eng. Chem. Fundamentals 8, 144 (1969a).

Sweed, N. H., and Wilhelm, R. H., Ind. Eng. Chem. Fundamentals 8, 221 (1969).

Tudge, A. P., Can. J. of Physics 40, 557 (1962).

Zhukhovitskii, A. A., Zolotareva, O. V., Sokolov, V. S., Turkeltaub, N. M.,

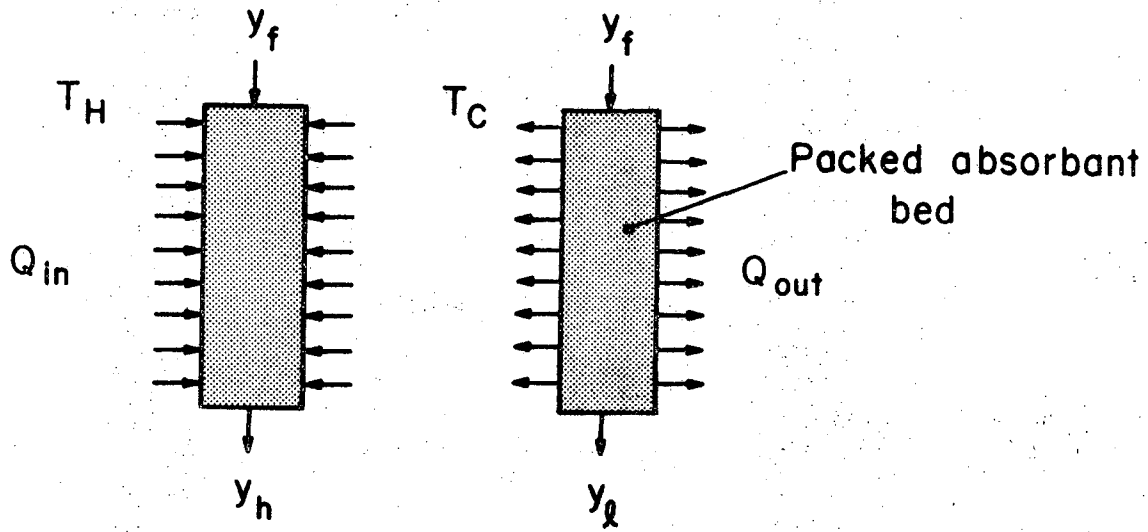
Doklady Akad. Nauk SSSR 77, 453 (1951).

Zhukhovitskii, A. A., "Gas Chromatography," Third Symposium, Edinburgh, edited

by R. P. W. Scott, Butterworth Scientific Publications, London, 1960.

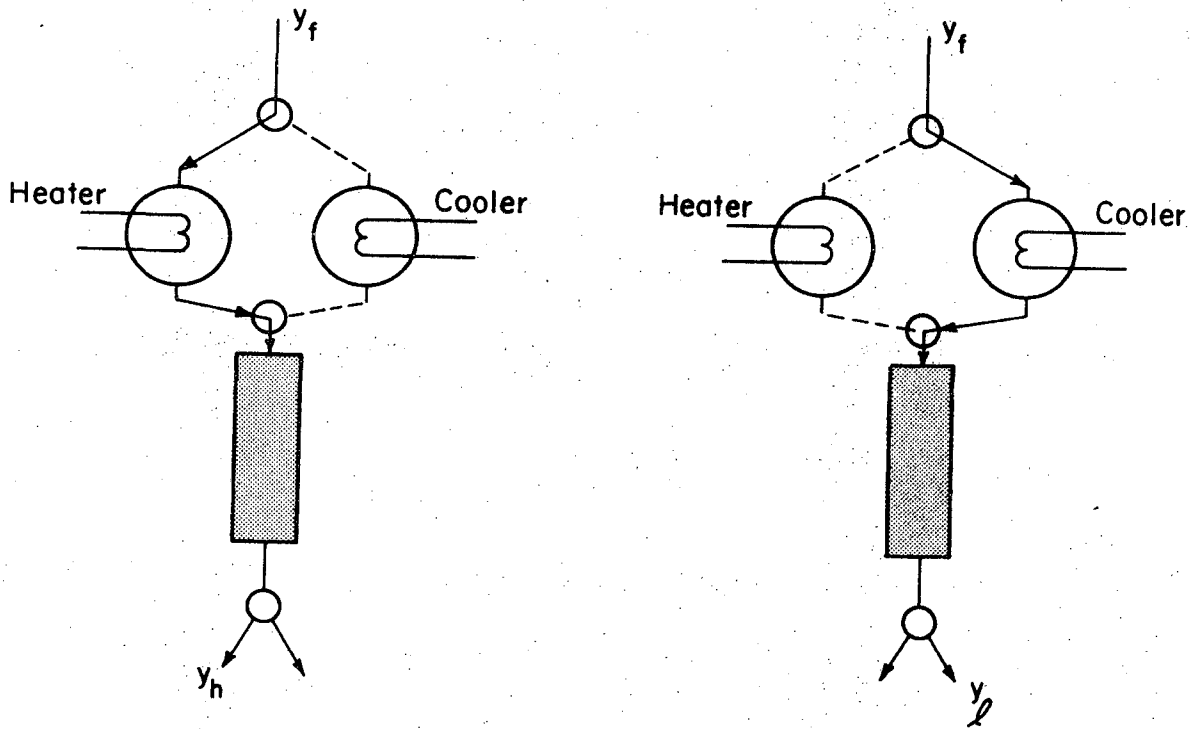
LIST OF FIGURES

- Fig. 1. Single-zone operation of cycling zone adsorber.
- Fig. 2. Characteristic lines used in Equilibrium Theory for linear isotherms--single zone, square-wave cycling.
- Fig. 3. Characteristic lines used in Equilibrium Theory for linear isotherms--multiple zones, square-wave forcing.
- Fig. 4. Equilibrium Theory solution for non-linear isotherms--two zones, square-wave forcing.
(a) characteristic lines; (b) effluent concentrations vs. time.
- Fig. 5. Characteristic lines showing possible interactions between thermal waves and concentration waves--step forcing.
- Fig. 6. Column-section arrangement for dual-zone experiments.
- Fig. 7. Effluent concentration profile for a single zone, standing thermal wave.
- Fig. 8. Effluent concentration profile for a single zone and a standing thermal wave--effect of feed concentration.
- Fig. 9. Separation factors for single-zone operation with standing thermal waves--effect of frequency.
- Fig. 10. Comparison of standing- and travelling-wave step forcing on a single-zone system.
- Fig. 11. Comparison of single- and dual-zone standing, square-wave forcing.
- Fig. 12. Comparison of standing and travelling square-wave forcing using two zones.



Heating half-cycle

Cooling half-cycle

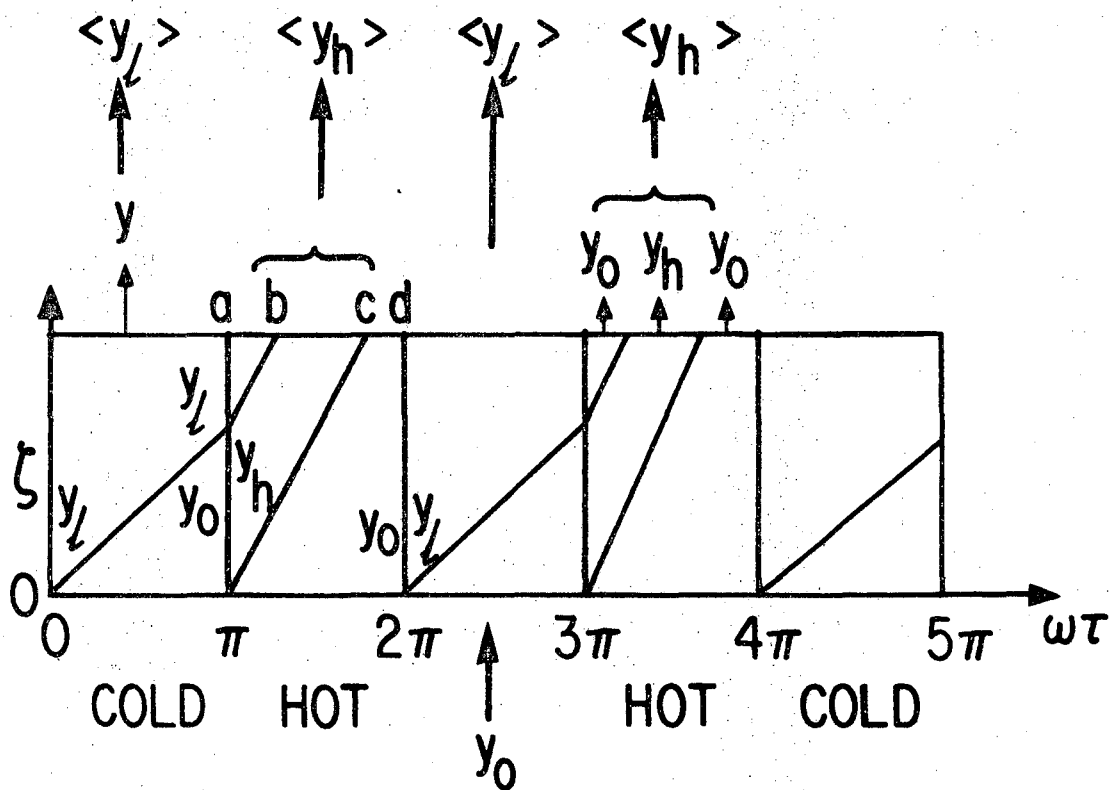


First half-cycle

Second half-cycle

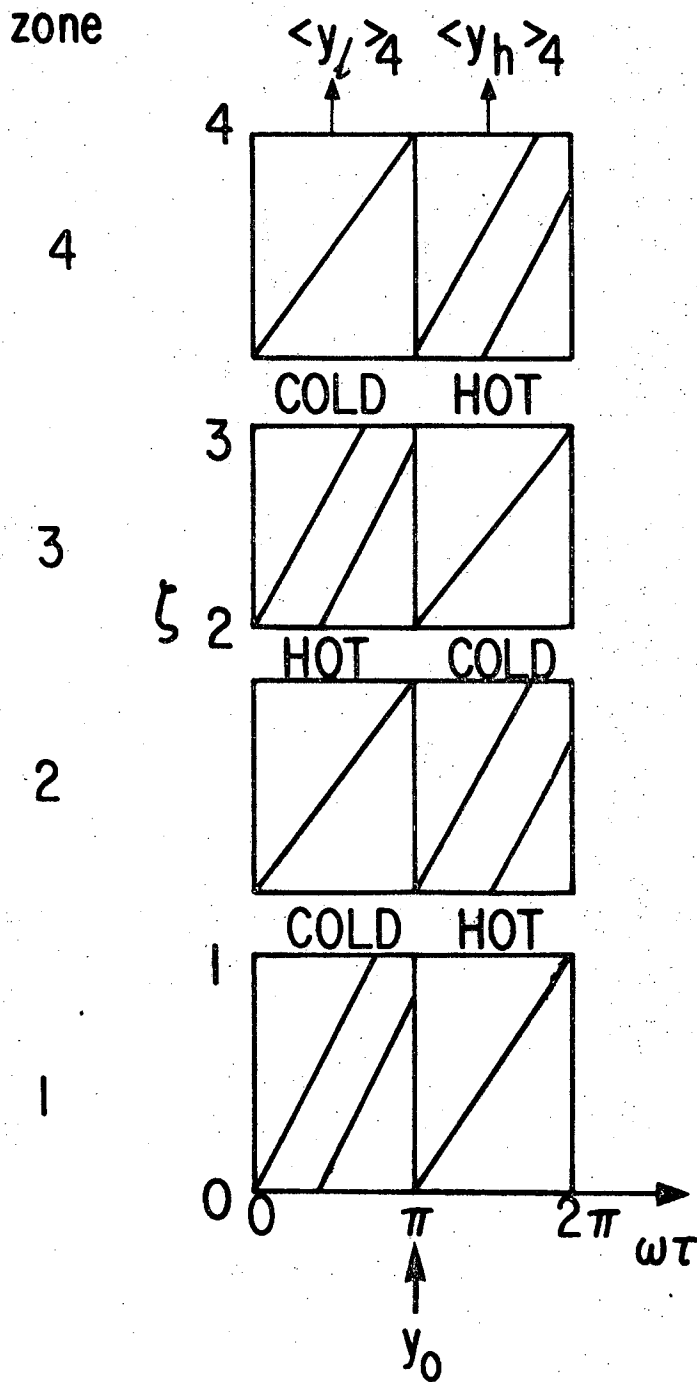
XBL694 - 2398

Fig. 1. Single-zone operation of cycling zone adsorber.



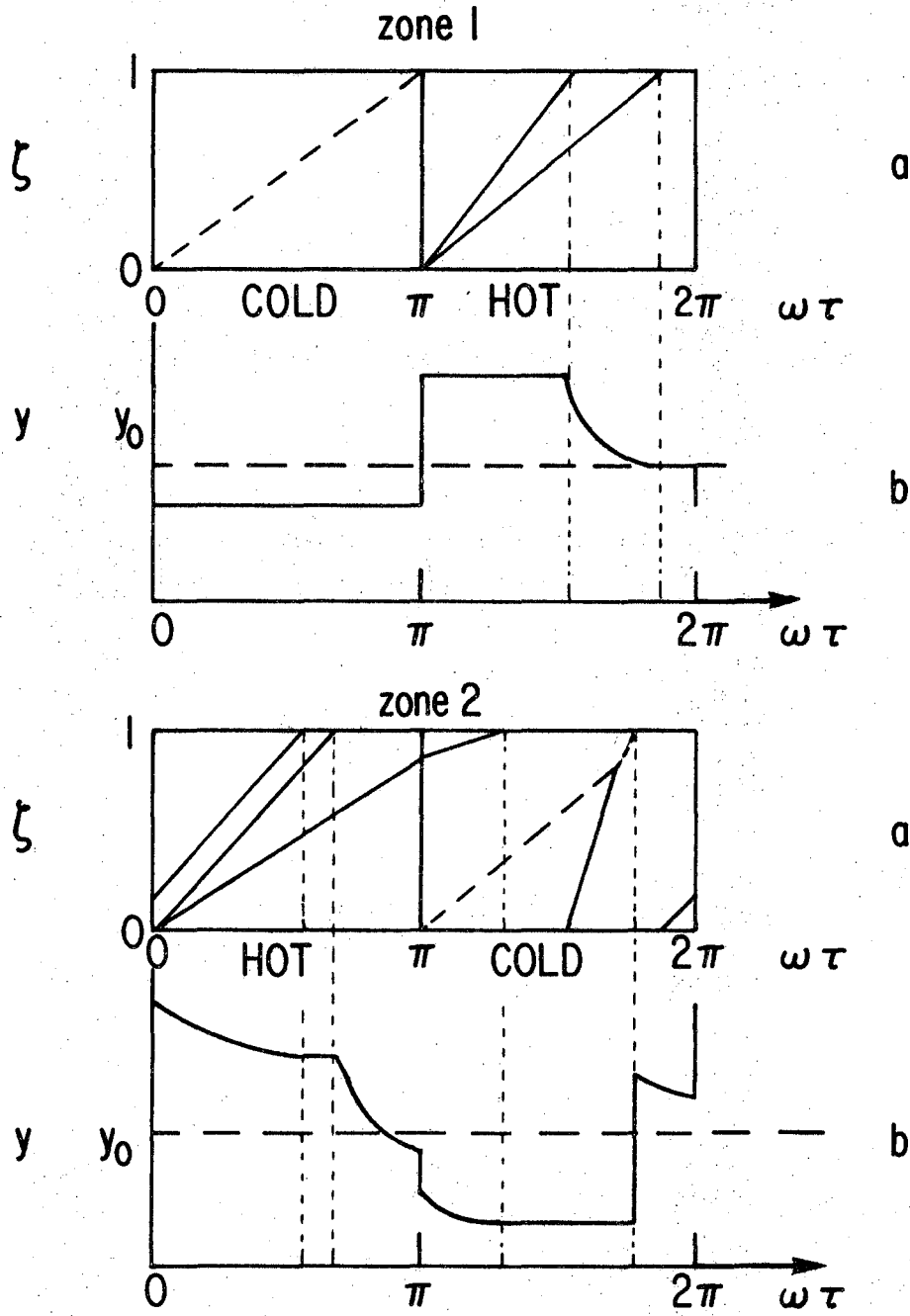
XBL 697-937

Fig. 2. Characteristic lines used in Equilibrium Theory for linear isotherms-single zone, square-wave cycling.



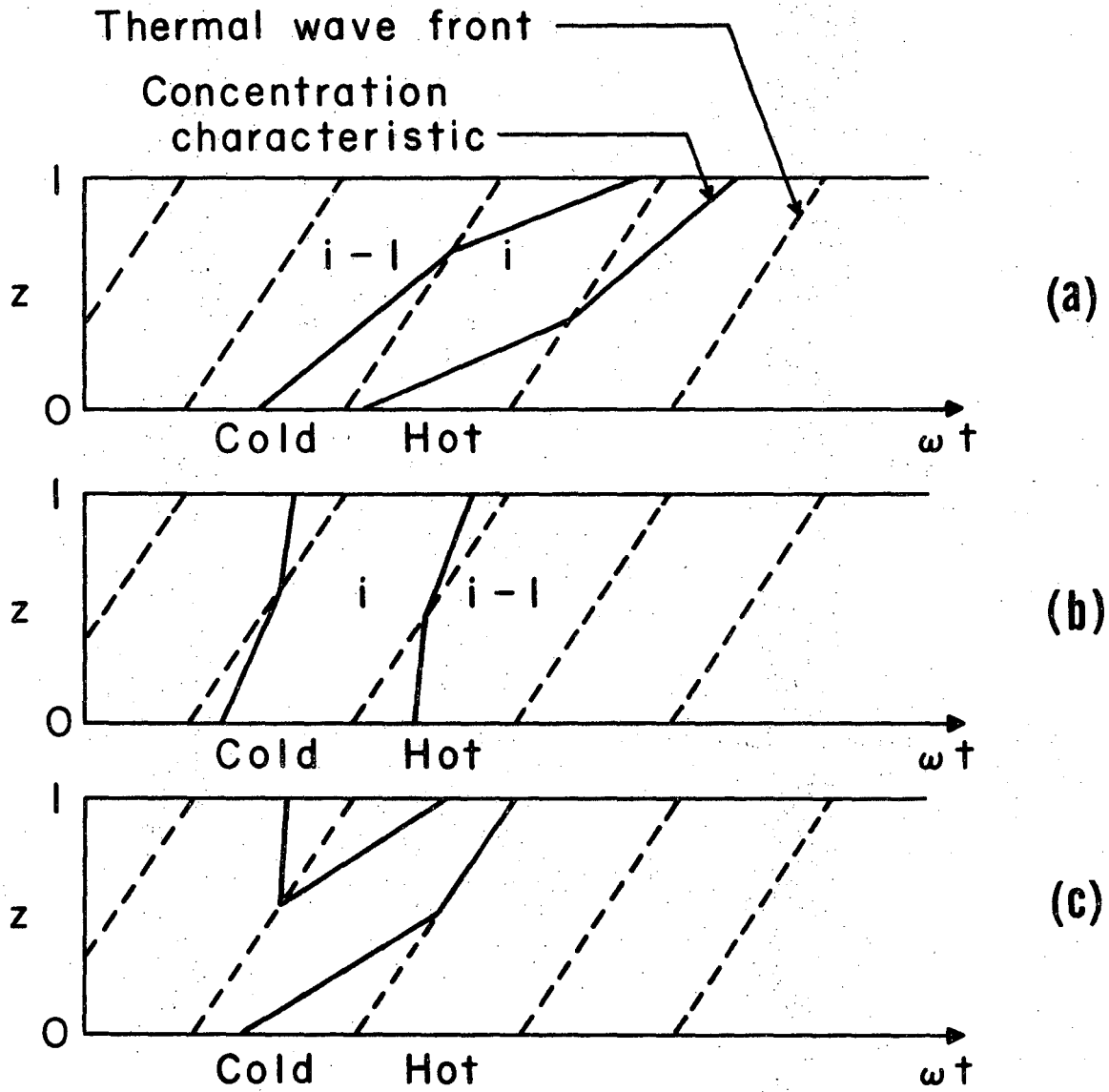
XBL 697-938

Fig. 3. Characteristic lines used in Equilibrium Theory for linear isotherms-multiple zones, square-wave cycling.



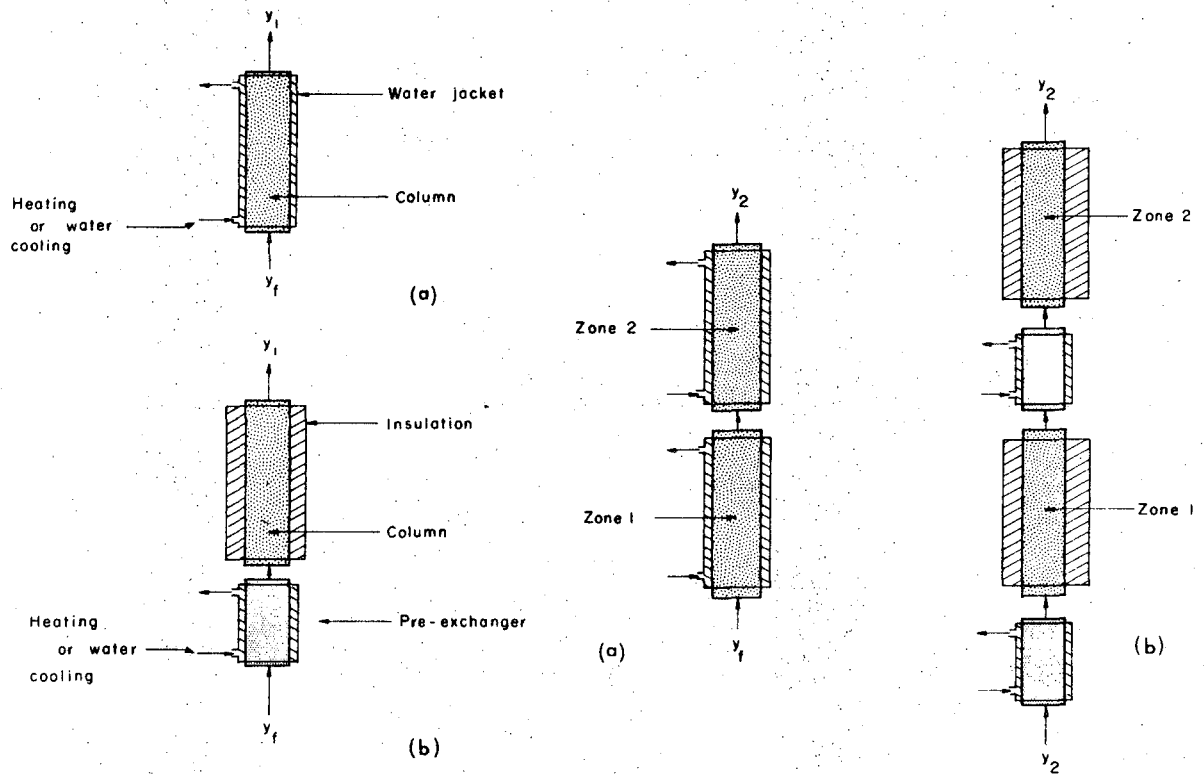
XBL 697-940

Fig. 4. Equilibrium Theory solution for non-linear isotherms--two zones, square-wave forcing. (a) characteristic lines; (b) effluent concentrations vs. time.



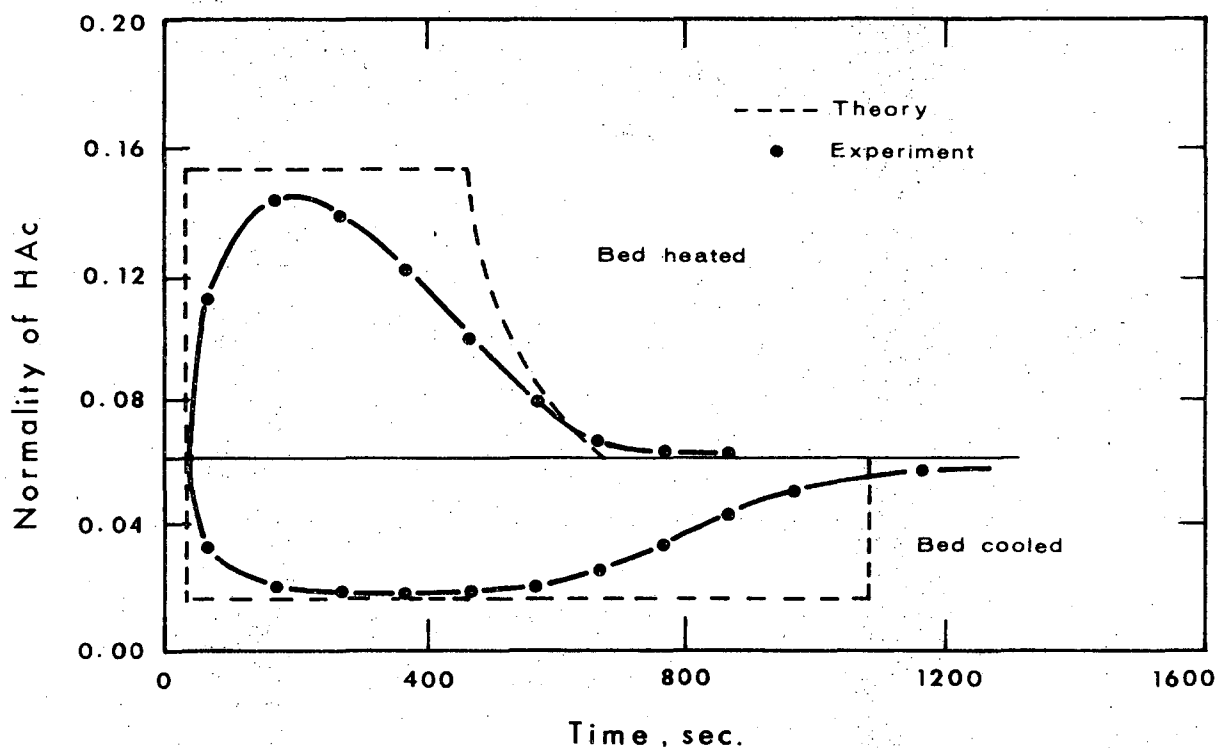
XBL 697-1049

Fig. 5. Characteristic lines showing possible interactions between thermal waves and concentration waves--step forcing.



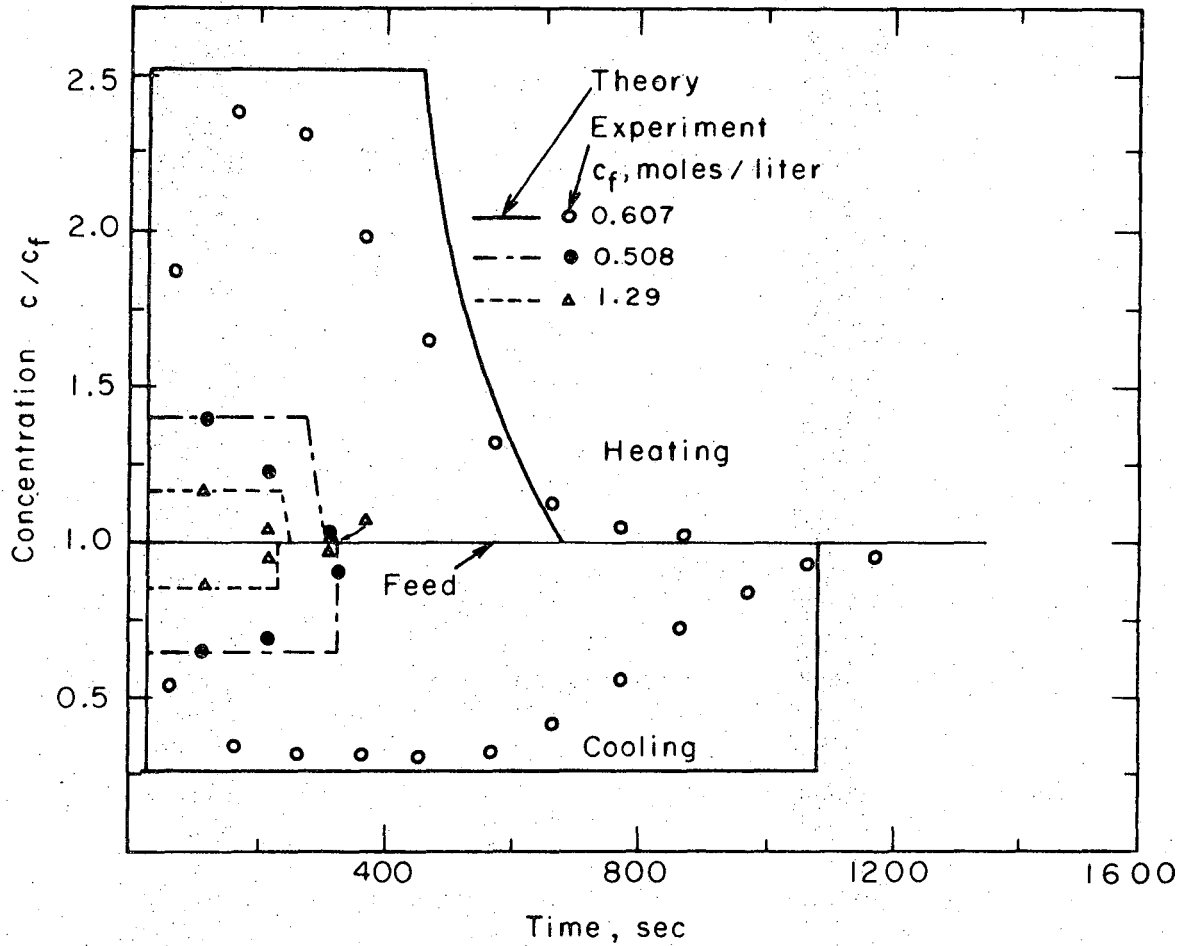
XBL 708-1749

Fig. 6. Column-section arrangement for dual-zone experiments.



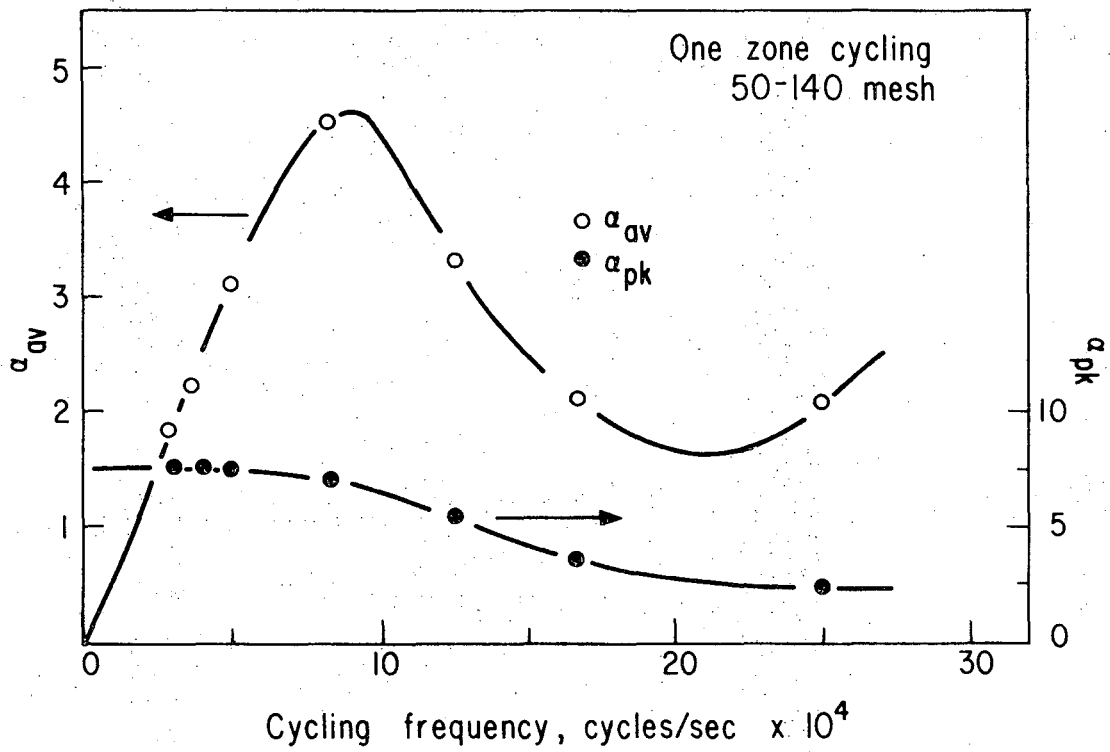
XBL 697-962

Fig. 7. Effluent concentration profile for a single zone, standing thermal wave.



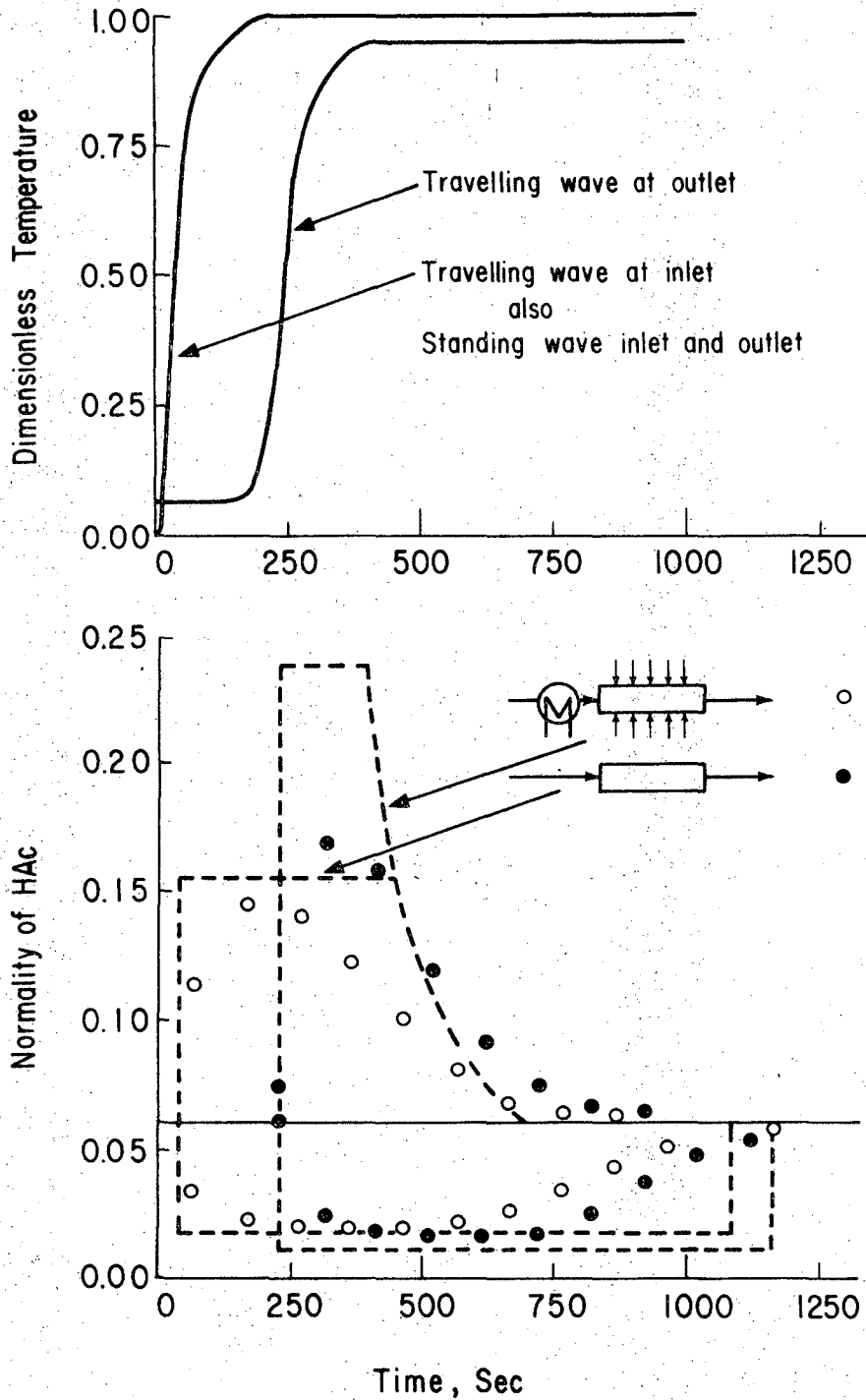
XBL 697-973

Fig. 8. Effluent concentration profile for a single zone and a standing thermal wave--effect of feed concentration.



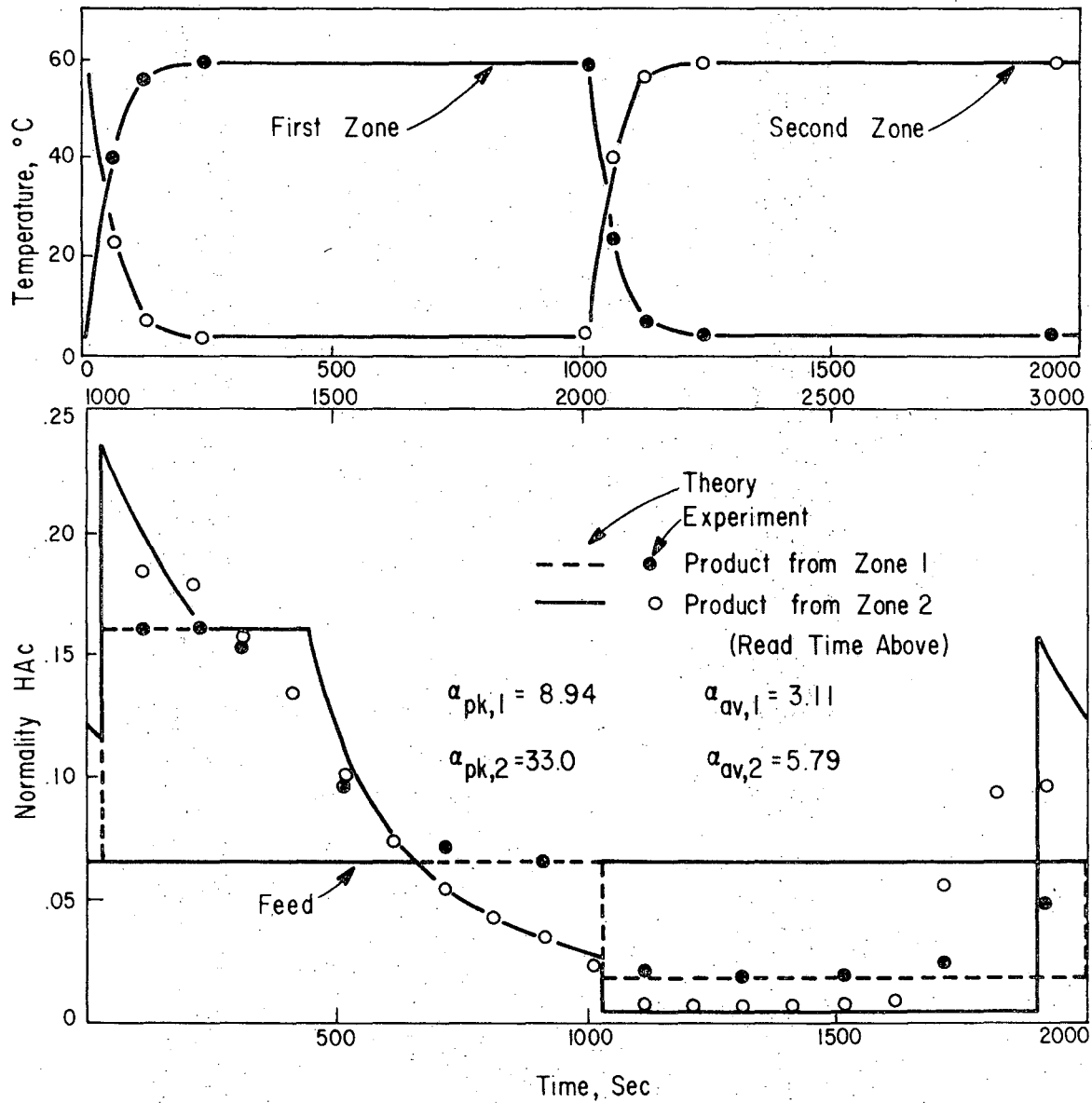
XBL 697-963

Fig. 9. Separation factors for single-zone operation with standing thermal waves--effect of frequency.



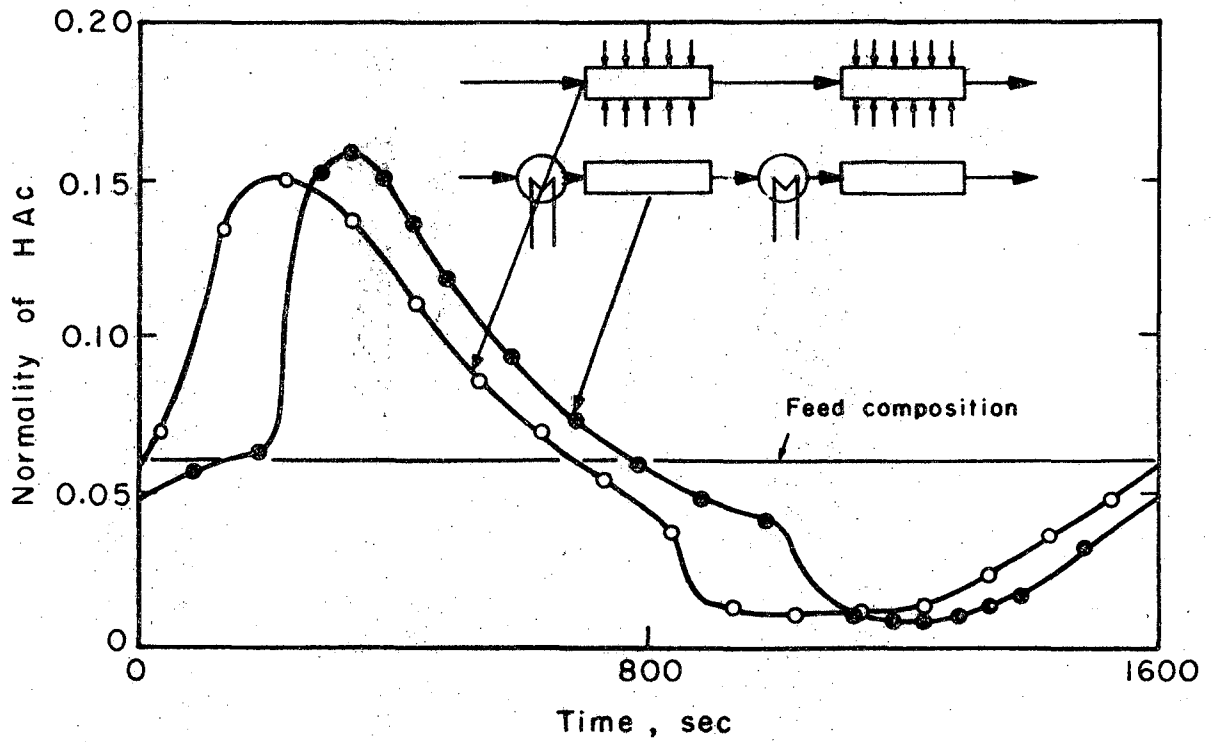
XBL 697-964

Fig. 10. Comparison of standing- and travelling-wave step forcing on a single-zone system.



XBL 697-965

Fig. 11. Comparison of single- and dual-zone standing, square-wave forcing.



XBL 697-976

Fig. 12. Comparison of standing and travelling square-wave forcing using two zones.

LEGAL NOTICE

This report was prepared as an account of Government sponsored work. Neither the United States, nor the Commission, nor any person acting on behalf of the Commission:

- A. Makes any warranty or representation, expressed or implied, with respect to the accuracy, completeness, or usefulness of the information contained in this report, or that the use of any information, apparatus, method, or process disclosed in this report may not infringe privately owned rights; or*
- B. Assumes any liabilities with respect to the use of, or for damages resulting from the use of any information, apparatus, method, or process disclosed in this report.*

As used in the above, "person acting on behalf of the Commission" includes any employee or contractor of the Commission, or employee of such contractor, to the extent that such employee or contractor of the Commission, or employee of such contractor prepares, disseminates, or provides access to, any information pursuant to his employment or contract with the Commission, or his employment with such contractor.

TECHNICAL INFORMATION DIVISION
LAWRENCE RADIATION LABORATORY
UNIVERSITY OF CALIFORNIA
BERKELEY, CALIFORNIA 94720